Fiber Design For High-Power Low-Cost Yb:Al-Doped Fiber Laser Operating at 980 nm

J. Kim, Daniel B. S. Soh, Johan Nilsson, David J. Richardson, and Jayanta K. Sahu

***Abstract*—We investigated an Yb:Al-doped depressed-clad hollow optical fiber (DCHOF) for cladding-pumped 980-nm laser operation. With a careful design, the nonzero fundamental-mode cutoff characteristics of a DCHOF allows the competing 1030–1060 nm emission to be filtered out, despite being quite close to 980 nm. The laser yielded over 3 W of output power in a diffraction limited beam ($M^2 \sim 1.09$) from a DCHOF with an inner-cladding diameter of 120 μm. This is large enough for pumping with standard fiber-coupled multimode diode sources. By reducing the inner-cladding size to 90 μm, and hence, lowering the 980-nm threshold, the output power was scaled up to 7.5 W. However, we believe that the M^2-parameter degrades to 2.7, as a result of increased cladding-mode lasing, as the cladding thickness is reduced.**

***Index Terms*—Optical fiber fabrication, optical fiber lasers, Ytterbium.**

I. Introduction

HIGH-POWER single-mode 980-nm lasers can be used for pumping of erbium-doped fiber amplifiers and lasers [1], [2], as well as for blue light generation by frequency doubling [3]–[5]. Commercially available single-mode 980-nm laser diodes are not only limited in output power but are expensive, too. As an alternative, high-power Yb-doped fiber (YDF) sources operating at 980 nm was demonstrated using a jacketed air clad (JAC) structure [4], [6]. These can be scaled to several watts of output and can also be used as amplifiers [4], considerably offering higher peak powers when pulsed [14] than the diodes. They are pumped by multimode laser diodes at around 915 nm. As explained in [5], the high numerical aperture (NA) and the small inner-cladding (30-μm diameter in [6]) help to improve the efficiency. It becomes easier to reach the laser threshold, which is relatively high. As the emission and absorption cross sections are comparable at 980 nm, at least ~50% of the Yb-ions need to be excited. An even more important point is the reduction in the inner-cladding to core area ratio that the small inner cladding brings about. To suppress unwanted amplified spontaneous emission (ASE) in a broad wavelength range of around 1030–1060 nm, which can experience high levels of gain at excited Yb-ion fractions of less than 50%, the area ratio must be small [7]. Therefore, as limits on inner-cladding NA and core size are reached, it is not possible to scale the output power of a 980-nm Yb-doped fiber laser (YDFL) of this type by scaling the inner-cladding area, even when the pump diode brightness and the pump intensity in the fiber are much higher than needed to invert the Yb-ions. Rather, diode sources of much higher brightness are required for further power scaling. Unfortunately, high-brightness diode sources are more expensive and less efficient than less bright sources of the same output power. An alternative approach for achieving a high-power 980-nm YDFL would be to design the waveguide structure such that it acts as a distributed filter along the fiber. A distributed filter can remove spontaneous emission at 1030–1060 nm before it is amplified, and thereby, suppress power losses to ASE. This relaxes the requirements on the area ratio, so that the inner cladding can be made larger. However, the undesired emission is quite close to the laser wavelength, which makes it challenging to reach sufficient filter sharpness.

In this paper, we investigate a depressed-clad hollow optical fiber (DCHOF) structure [8, Fig. 2] for this purpose. The fiber is designed for cladding-pumped 980-nm laser operation, and comprises of a ring-shaped core around an air hole in the center of the fiber, and a ring-shaped depressed cladding region around the core. The nonzero fundamental (LP_{01}) mode cutoff characteristic of such a waveguide structure was used to suppress the undesired ASE at wavelengths around 1030 nm and longer, along the fiber. We found that it was indeed possible to achieve sufficient filter sharpness with a carefully designed and fabricated fiber, and we discuss the details and tradeoffs of this method. Experimentally, we obtained 3.1 W of output power in a diffraction limited beam $M^2 \sim 1.09$. However, with a degraded M^2 of 2.7, this increased to 7.5 W when the inner-cladding diameter was reduced from 120 to 90 μm. The other parameters of the fiber cross section remained the same. The corresponding slope efficiencies of the two fibers, with respect to launched pump power were 34% and 49%, respectively. The larger inner cladding of the DCHOF, compared to the previous JAC fiber [4], [6] (without any waveguide filter), enable the use of a high-power pump source of relatively low brightness. In particular, the DCHOF is compatible with standard high-power fiber-coupled multimode pump sources, which opens up for scaling of the 980-nm power in a cost effective way.

This paper is organized as follows. We discuss the requirements of a cladding-pumped 980-nm YDFL in Section II. We introduce the DCHOF in Section III. We investigate how well the DCHOF design can satisfy the 980-nm YDFL requirements and optimize the design. We then consider the properties of a DCHOF that we fabricated, first theoretically and then, experimentally. This includes the wavelength filtering properties of bending loss. We finally present and discuss experimental results on 980-nm laser operation in Section IV.

Manuscript received November 11, 2006; revised March 28, 2007.

The authors are with the Optoelectronics Research Center, University of Southampton, Highfield, Southampton SO16 3PU, U.K. (e-mail: dbs@calmaropt.com; jn@orc.soton.ac.uk; djr@orc.soton.ac.uk; jks@orc.soton.ac.uk).

Digital Object Identifier 10.1109/JSTQE.2007.896628

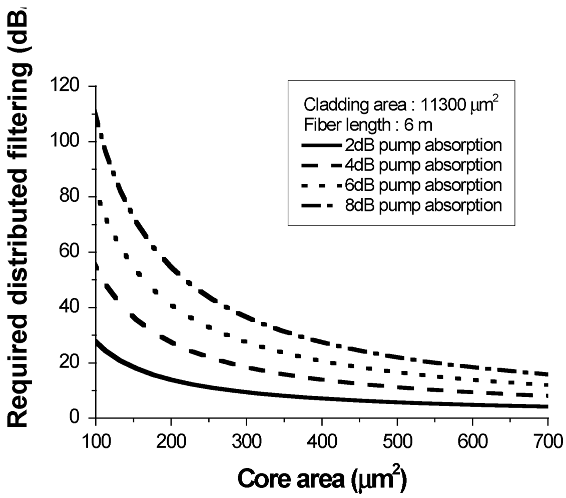

Fig. 1. Required distributed filtering for complete suppression of the gain at 1030 nm as a function of the core area at several operating pump absorptions. Cladding area is 11300 μm^2 (120-μm diameter) and fiber length is 6 m.

II. Requirements for a 980-nm YDFL

In order to realize an YDFL operating at 980 nm, the competing stimulated emissions at the longer wavelength (1030–1060 nm) in YDF should be suppressed. 1030 nm is a particularly important wavelength because the gain peaks there and it is close to 980 nm. From [7], the undesired gain at 1030 nm, in logarithmic units, is given by

$$G_{1030} \sim 0.25 G_{980} + 0.72 \eta \alpha_p \tag{1}$$

where G_{1030} and G_{980} are the gain at 1030 nm and 980 nm, respectively, $\eta = A_{\rm clad}/A_{\rm co}$, is the cladding to core area ratio, and α_p is the operating pump absorption. It is assumed that each pump mode sees the same absorption, equal to the core absorption divided by the area ratio. Although each cladding mode experiences a different characteristic absorption, a practical well-designed cladding-pumped fiber should exhibit uniform absorption along its length owing to a combination of mode scrambling techniques and special geometric fiber designs. The constants in (1) depend on the absorption and emission cross sections, and can be considered typical for YDFs at these wavelengths. For a laser oscillator with 100% reflectivity at one end and 4% reflectivity at the other end of the cavity, the total round-trip losses are 14 dB, where we neglect the background loss of the fiber. For lasing, we need $G_{980} = 7$ dB. For example, consider the fiber with 120-μm cladding diameter (cladding area 11300 μm^2). The area ratio η depends on the core area. If a 300-μm^2 core area is considered, $\eta = 37.6$. Then, the unwanted gain at 1030 nm becomes $1.75\,{\rm dB} + 27.2\alpha_p$. Under these conditions, every decibel of the pump absorption contributes 27.2-dB gain at 1030 nm. In practice, this would restrict the operating pump absorption to 1–2 dB, which is insufficient for efficient operation. Compared to this, the contribution of the 980-nm gain [the first term in (1)] is unimportant. Fig. 1 shows the filtering required to suppress the net gain to 0 dB at 1030 nm depending on the core area for an inner-cladding area of 11300 μm^2. The 980-nm gain is assumed to be 1.2 dB/m or 7 dB in a 6-m-long fiber. The larger the core area, the smaller the area ratio, and the smaller the suppression needed. However, a too large core leads to a multimode output beam. Although up to $\sim$40 dB of gain at 1030 nm can be accepted before spurious lasing and high-power ASE become unavoidable, it is still clear that for acceptable single-mode core areas of up to 300 μm^2, the 1030-nm gain would have to be suppressed along the fiber. We should not forget, however, that these values depend strongly on the spectroscopic cross sections, which will be different in fibers of different composition than what is assumed in [7].

In Fig. 1, if the fiber length is 6 m and the operating pump absorption is 4 dB, then $\sim$17-dB/m distributed filtering loss at 1030 nm is required for a 300-μm^2 core area. A higher pump absorption will require a higher filtering loss per unit length, insofar as the fiber length is fixed. It should be realized that in order to fix the fiber length to 6 m as shown in Fig. 1, the Yb-concentration of the fiber has to be changed to obtain the different pump absorptions. As the Yb-excitation level will be close to 50% in a 980-nm YDFL, the operating pump absorption per unit length will be slightly less than half of the unpumped absorption with all the ions in the ground state, and measured, e.g., with a low pump power. Thus, an operating absorption of 8 dB in a 6-m-long fiber implies that the unpumped pump absorption should be $\sim$2.7 dB/m. This would also fix the Yb-concentration of the fiber.

Given a specific Yb-concentration and cross-sectional data, it is also straightforward to calculate the unwanted gain at 1030 nm at 50% Yb-excitation. For example, at a Yb concentration of 3000 ppm by weight, it becomes 34 dB/m using the cross sections of [7]. It follows that points in Fig. 1 with the same required distributed filtering correspond to fiber designs with similar Yb concentrations, with slight differences resulting from slight differences in the Yb-excitation. We can also assess the tolerable loss at 980 nm. In order to keep the efficiency close to the theoretical maximum, the loss should be less than 1 dB, which is very less than 0.2 dB/m in a 5–6-m-long fiber.

If the Yb-concentration is reduced with a fixed area ratio, the required 1030-nm filtering loss per unit length becomes lower. To obtain a given operation pump absorption, it is then necessary to use a longer fiber. The total 1030-nm filtering loss will be the same. As the total tolerable loss at 980 nm also stays the same, the acceptable loss per unit length becomes smaller.

On the other hand, if the area ratio is reduced with a fixed Yb-concentration, the pump absorption increases so that a shorter fiber can be used, and a higher loss at 980 nm can be tolerated. This relaxes the differences in loss between 980 nm and 1030 nm that a filter must provide, i.e., it relaxes the requirements on the filter sharpness.

Thus, different Yb-concentrations, area ratios, and operating pump absorptions lead to different requirements on the 1030-nm suppression and the tolerable 980-nm loss, as it comes to total values (over the whole fiber) as well as per unit length. It also affects the relation between the acceptable 980-nm fiber loss and required 1030-nm loss, i.e., the filter sharpness. Key is to find a fiber design that can satisfy the filter requirements in a fiber with a sufficiently large inner cladding for scaling to high powers and a pump absorption sufficiently large for a high efficiency. Both the filter requirements and the filter characteristics depend on the fiber design.

The threshold is also important for efficient operation. A 980-nm YDFL requires that ~50% of the ions are excited to reach gain. The threshold in terms of absorbed pump power becomes

$$p_{\text{abs}}^{\text{th}} = \frac{h\nu_p \sigma_a^s}{\tau \sigma_a^p (\sigma_e^s + \sigma_a^s)} A_{\text{clad}} \alpha_{\text{ss}}^p = (0.178\,\text{mW}/\mu\text{m}^2) A_{\text{clad}} \alpha_{\text{ss}}^p \tag{2}$$

where $h\nu_p$ is the pump photon energy $\tau = 0.76$ ms is the fluorescence lifetime, $\sigma_e^s = 25.8 \times 10^{-25}$ m^2 and $\sigma_a^s = 25.7 \times 10^{-25}$ m^2 are the emission and absorption cross sections at the signal wavelength, $\sigma_a^p = 8.25 \times 10^{-25}$ m^2 is the absorption cross section at the pump wavelength (915 nm), and α_{ss}^p is the pump absorption in nepers with all the Yb-ions in the ground state. If $\alpha_{\text{ss}}^p = 3.8$ Np or 16.5 dB, the operating pump absorption α_p becomes 8 dB, which is a reasonable value. Thus, with an inner-cladding area A_{clad} of 11300 μm^2, $P_{\text{abs}}^{\text{th}}$ becomes 7.65 W. This is actually the absorbed pump power required to bleach the 980-nm absorption, whereas a marginally higher absorbed pump power will be needed to create the gain needed for lasing. Furthermore, a pump absorption of 8 dB implies a pump leakage of 16%. Even with these minor adjustments, the laser threshold would be less than 10 W of launched pump power. This is a reasonable threshold, given that 915-nm diode pump sources with 30–40 W of power from a 0.22-NA 100-μm core diameter fiber pigtails are currently commercially available. Thus, even with an inner-cladding diameter of 120 μm, the threshold of a 980-nm YDFL is not prohibitively large. The challenge is rather to implement a filter that provides a high loss at 1030-nm without inducing excessive loss at 980 nm.

It is worth pointing out that the very low-saturation intensity of 980-nm YDFLs make it very easy to overcome (excess) losses at 980 nm, e.g., from bending or any other cavity losses. It only takes 3.8 mW of absorbed pump power to increase the gain by 1 dB with a core area of 300 μm^2. This is much smaller than the laser threshold. Although the impact on the threshold is small, the impact on the slope efficiency can still be severe.

The low saturation intensity makes it possible to create gain for cladding modes as well. The gain slope for cladding modes become 6.9 dB/W on average with an inner-cladding area of 11300 μm^2, but it will be significantly higher for cladding modes with high overlap with the core.

III. Design of Yb-Doped DCHOF for 980-nm Operation

DCHOFs have been used in the past for cladding-pumped 0.9-μm Nd-doped fiber lasers [8], [9] in which competing 1060-nm emission needs to be filtered out. However, much smaller wavelength spacing between the desired laser emission and the competing emission makes this much more challenging in case of the 980-nm YDFL, and calls for careful fiber design and fabrication. The modal characteristics of the DCHOF were numerically analyzed to determine the fiber parameters suitable for 980-nm laser operation. Assuming the weakly guiding condition and linearly polarized (LP) modes, the radial dependence of the transverse field component in the DCHOF is

$$E(r) = \begin{cases} A_0 I_m(vr) \\ A_1 J_m(ur) + A_2 Y_m(ur) \\ A_3 I_m(wr) + A_4 K_m(wr) \\ A_5 K_m(sr) \end{cases} \tag{3}$$

where r is the radial position, $A_i (i = 0, 1, 2, 3, 4, 5)$ are constants, J_m and Y_m are Bessel functions of order m of the first and second kind, respectively, and I_m and K_m are modified Bessel functions of the first second kind. The mode parameters ν, u, w and s are defined as $v = \sqrt{\beta^2 - k_0^2}, u = \sqrt{n_{\text{co}}^2 k_0^2 - \beta^2}, w = \sqrt{\beta^2 - n_{\text{dip}}^2 k_0^2}$, and $s = \sqrt{\beta^2 - n_{\text{clad}}^2 k_0^2}$, where β is the propagation constant of the mode, and k_0 is the vacuum wave number. The parameters $n_{\text{co}}, n_{\text{dip}}$, and n_{clad} are the refractive indices of the core, depressed region, and the silica cladding, respectively. The propagation constant β of a mode is found as a solution to a characteristic equation. By applying the boundary conditions, i.e., that the transverse field component and its radial derivative are continuous at the three boundaries, $r = r_{\text{air}}, r = r_{\text{co}}$, and $r = r_{\text{dip}}$ respectively, the characteristic equation can be obtained as shown in (4) at the bottom of the page.

Using a numerical solution technique (e.g., a Newtonian method), the propagation constant β that satisfy the characteristic equation in (4), can be obtained. This eigenvalue β determines the modal fields through (3). The propagation constant is related to the effective index (n_{eff}) of a mode by the relation $n_{\text{eff}} = \beta/k_0$, where k_0 is the wavenumber in free space. For DCHOFs of appropriate parameters and sufficiently large wavelengths, there is no solution to the characteristic equation, which means that there is no guided mode. In such fibers, the fundamental mode is the first to become guided, as the wavelength is reduced beyond some value, i.e., the cutoff wavelength. Since longer unguided wavelengths are rejected, the fiber acts as a short-pass filter. We are primarily interested in fibers and wavelength ranges in which either no mode or a single mode is guided.

In order to filter out emission at wavelengths of 1030 nm and longer, one can set the fundamental mode cutoff wavelength between 980 and 1030 nm. However, because of the small difference between these wavelengths, the effective index at 980 nm becomes too small, which causes significant microscopic and

$$\begin{bmatrix} I_m(Vr_{\text{air}}) & -J_m(ur_{\text{air}}) & -Y_m(ur_{\text{air}}) & 0 & 0 & 0 \\ VI_m^1 vr_{\text{air}}) & -uJ_m^1 ur_{\text{air}}) & -uY_m^1 ur_{\text{air}}) & 0 & 0 & 0 \\ 0 & J_m(ur_{\text{co}}) & Y_m(ur_{\text{co}}) & -I_m(wr_{\text{co}}) & -K_m(wr_{\text{co}}) & 0 \\ 0 & 0 & -uJ_m^1(ur_{\text{co}}) & -uY_m^1(ur_{\text{co}}) & -wI_m^1(ur_{\text{co}}) & -wK_m^1(ur_{\text{co}}) \quad 0 \\ 0 & 0 & 0 & I_m(wr_{\text{dip}}) & K_m(wr_{\text{dip}}) & -K_m(sr_{\text{dip}}) \\ 0 & 0 & 0 & wI_m^1(wr_{\text{dip}}) & wK_m^1(wr_{\text{dip}}) & -sK_m^1(sr_{\text{dip}}) \end{bmatrix} = 0. \tag{4}$$

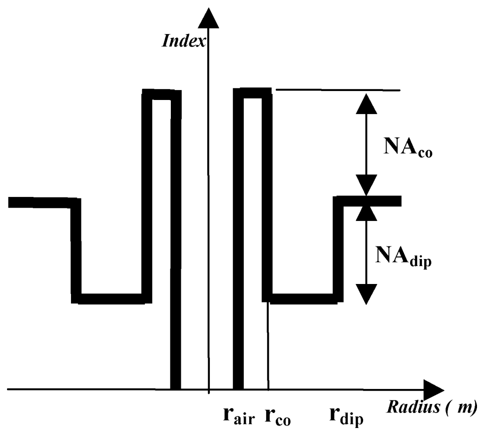

Fig. 2. Schematic refractive index structure of the DCHOF (thickness $= r_{\rm co} - r_{\rm air}$).

macroscopic bending loss there [10]. In practice, these factors make the effective cutoff wavelength shorter than the theoretical one. In order to increase the effective index at 980 nm and to reduce the bending loss, the theoretical fundamental mode cutoff wavelength should be set somewhat longer than 1030 nm, but sufficiently close to 1030 nm so that this wavelength is effectively cut off by a high bending loss. In practice, we are really looking for fiber designs with a large bending loss at 1030 nm and a low bending loss at 980 nm, under the right bending conditions. In this paper, we consider initially a DCHOF with a theoretical fundamental mode cutoff at 1150 nm, which we found to be a good choice. By a controlled coiling of the fiber, we can then optimize the bending-loss characteristics for 980-nm laser operation. Based on [10], we calculated the theoretical macroscopic bending loss for light propagating in the core for fibers with different parameters but with a nearly fixed cutoff wavelength of 1150 nm.

Fig. 2 shows the schematic refractive index structure of the DCHOF. There are five parameters, each of which affect the cutoff wavelength, so that there are four independent variables when the cutoff wavelength is fixed to 1150 nm. For simplicity, we will not investigate the whole parameter space, but only use the numerical aperture of the core ${\rm NA}_{\rm co} = \sqrt{n_{\rm co}^2 - n_{\rm clad}^2}$ as a single independent variable. The hole radius is fixed to 5 μm and ${\rm NA}_{\rm dip} = \sqrt{n_{\rm clad}^2 - n_{\rm dip}^2}$ is fixed to 0.08. This hole size and index depression allow for reliable fabrication of DCHOFs. The thickness of the ring-core was adjusted to yield a cutoff wavelength of approximately 1150 nm. The thickness of the depressed clad was set to twice the thickness of the ring. Table I presents the parameters and the $\rm LP_{01}$ mode cutoff wavelength of specific fiber designs of different core NAs. The fabrication tolerance of the core thickness and the depressed clad is 2%, which cause a deviation of $\pm$30 nm at the fundamental mode cutoff wavelength depending on the core structure. As even relatively small variations in core thickness give rise to large variations of the fundamental mode cutoff wavelength, it is important to control accurately the fiber diameter in fiber drawing process. The tolerance of the hole size is not given in Table I, but it was found to be relatively large. However, as the hole size will

TABLE I
PARAMETERS OF SELECTED FIBER DESIGNS

No.	Core: Thickness ($r_{co} - r_{air}$) [m]	Core: NA	Depressed clad: Thickness ($r_{dip} - r_{co}$) [m]	Depressed clad: NA	Hole radius [m]	Core area (m^2)	LP_{01} mode cut-off wave-length [nm]
S1	9.10 (±0.18)	0.05	18.2 (±0.36)	0.08	5	546	1150 (± 30)
S2	7.30 (± 0.15)	0.06	14.6 (±0.29)	0.08	5	396	1150 (± 30)
S3	6.05 (± 0.12)	0.07	11.1 (±0.23)	0.08	5	305	1150 (± 30)
S4	5.15 (± 0.10)	0.08	10.3 (±0.20)	0.08	5	245	1150 (± 30)
S5	4.45 (± 0.09)	0.09	8.9 (±0.17)	0.08	5	202	1150 (± 30)

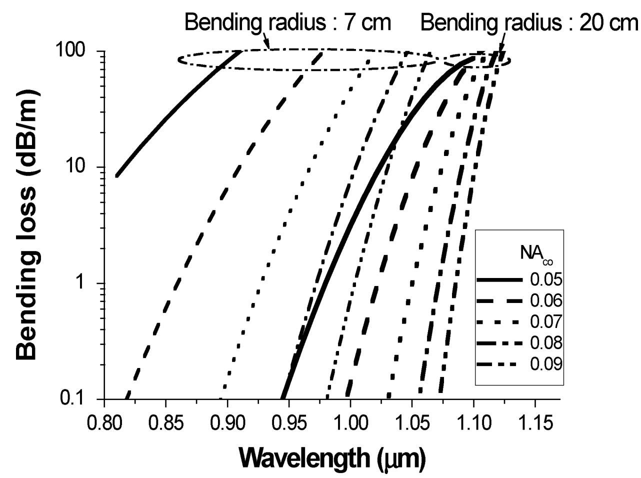

Fig. 3. Bending loss as a function of the wavelength for different $\rm NA_{co}$ fibers at 7- and 20-cm bending radius (according to Table I).

indirectly affect the core thickness when the fiber is drawn to a given diameter, the hole size must also be accurate in order to keep the cutoff wavelength fixed. A fiber diameter of 120 μm is considered initially.

Fig. 3 shows the macroscopic bending loss as function of wavelength for the different fiber parameters presented in Table I. The fiber was coiled with bending radii of 20 and 7 cm. Even though the theoretical cutoff wavelength is 1150 nm, the effective cutoff is shifted to shorter wavelengths. Smaller bending radii and lower core NAs result in shorter effective cutoff wavelengths. At 20-cm bending radius, a fiber with 0.05- or 0.06-core NA, or somewhere in between, may provide an appropriate effective cutoff wavelength according to these theoretical calculations. At 7-cm bending radius, the 0.09 core NA fiber appears more suitable. The other fibers would provide appropriate effective cutoff wavelengths at intermediate bend radii. However, it is also important that the fiber sharpness is sufficient. Fig. 3 shows that the higher NA fibers result in sharper cutoffs. On the other hand, the higher NA fibers have smaller cores, which according to Fig. 1, escalates the filter requirements.

Given these counteracting effects of a change in the core NA, we need to analyze and compare the effects of the NA on filter requirements and filter sharpness in more detail in order to

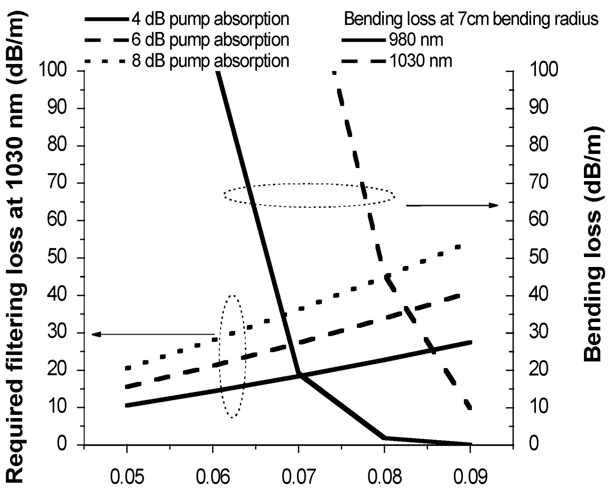

Fig. 4. Required filtering loss at 1030 nm and bending loss at two different wavelengths (980 and 1030 nm) for different pump absorptions and core NA (according to Table I) and 7-cm bending radius.

TABLE II
TOTAL LOSS AT 980-nm CORE NA AND Yb CONCENTRATION FOR DIFFERENT PUMP ABSORPTIONS AND FIBER LENGTHS WHEN THE BENDING RADIUS IS 7 CM. σp: PUMP ABSORPTION, $\alpha 980$: TOTAL LOSS AT 980 nm, NA_{co}: NA OF THE CORE, N_0: Yb CONCENTRATION

	Fiber length (m)								
	3			6			12		
σp	α_{980} (dB)	NA_{co}	N_0 (ppm)	α_{980} (dB)	NA_{co}	N_0 (ppm)	α_{980} (dB)	NA_{co}	N_0 (ppm)
4	5.4	0.081	4010	6	0.080	1960	1.2	0.089	1170
6	16.2	0.078	5640	7.2	0.082	3060	6	0.087	1690
8	26.1	0.075	7010	9.6	0.084	4280	8.4	0.085	2160

arrive at the optimum value. Fig. 4 shows the required filtering loss at 1030 nm for a 0-dB net gain together with the bending loss at the two key wavelengths, 980 and 1030 nm, versus core NA. The other core parameters were varied as well, when the core NA changed, as presented in Table I. The fiber length was 6 m. Thus, the curves for the required filtering loss are similar to those in Fig. 1, except that they are now plotted against the core NA rather than the core area. However, the core NA and core area are related, as shown in Table I. The bending-loss curves are plotted for a bending radius of 7 cm. For laser operation at 980 nm, the 1030-nm bending loss should be higher than the required 1030-nm filtering loss. This is the case for low NAs. However, if the NA is lower than necessary, then the 980-nm bending loss becomes higher than necessary. Therefore, the intersections between the curves for the 1030-nm bending loss and the required filtering loss correspond to the optimum fiber designs, for this particular fiber length and bending radius.

The loss at 980 nm corresponding to these intersections can then be determined from Fig. 4. For a more thorough optimization of the core NA, other bending radii (4, 7, and 15 cm) and fiber lengths (3, 6, and 12 m) were also considered. In all cases, 7 cm gave the lowest or close to the lowest, total loss at 980 nm, and therefore, we restrict further considerations to that bending radius. The total 980-nm bending losses are summarized in Table II for the different fiber lengths and operating pump absorptions, at 7-cm bending radius. We see that a fiber length of 12 m provides the lowest total loss at 980 nm for the three studied lengths, especially for low values (4 dB) of the total operating pump absorption. For higher values, the difference is smaller. Table II also specifies the optimum core NAs and Yb-concentrations for the different fiber lengths and pump absorption. In order to keep the 980-nm loss at an acceptable value, we should target an operating pump absorption of 4 dB or 60%.

Thus, we arrived at an optimum core design within the parameter space that we have examined. There are, however, several points to be noted. Our design gives us the minimum 980-nm loss, but the output power of a 980-nm YDFL will depend on the threshold. Furthermore, the pump absorption is on the low side. This can be increased by reducing the inner-cladding area at the expense of a more challenging pump launch. The optimum core parameters derived from our analysis would remain the same. An important point is that even though a 120-μm inner-cladding diameter has been assumed, this assumption only affects the operating pump absorption. The same optimum core designs would be obtained with a different inner-cladding size but with different pump absorptions.

In addition, a target of 0-dB total gain at 1030 nm is only approximately correct. With wavelength-selective cavity mirrors, (e.g., fiber Bragg gratings), a gain of at least 30 dB can be tolerated before strong ASE, and even spurious lasing become unavoidable. On the other hand, in order to avoid strong ASE, the 1030-nm gain must be sufficiently suppressed everywhere in the fiber, not just on average. Thus, strong unwanted ASE could possibly occur even with a 0-dB average gain.

Finally, bending loss depends strongly on fiber parameters, and is difficult to calculate accurately. A slight deviation in the shape of the core refractive index profile, for example, may result in a significant difference in the spectral characteristics of the bending loss.

The fiber we fabricated deviates slightly from the optimum design defined earlier. The fabricated fiber has a ring-shaped 5.7-μm-thick Yb-doped aluminosilicate core with 0.073-NA with respect to the silica cladding, around an air hole of 10-μm diameter, and an 11-μm thick depressed ring of $NA_{\text{dip}} = 0.08$ immediately outside the core. The core area becomes 280 μm^2. The depressed ring is surrounded by a pure-silica region, which dominates the inner cladding. The low-power pump absorption is 1.3 dB/m in a 120-μm inner-cladding diameter, corresponding to an Yb concentration of 1500 ppm by weight. Theoretically, the pump absorption becomes 0.6 dB/m at 50% Yb excitation.

Given these deviations, we next describe some additional calculated characteristics of a fiber with these parameters. We focus on whether the bending loss can provide sufficiently sharp

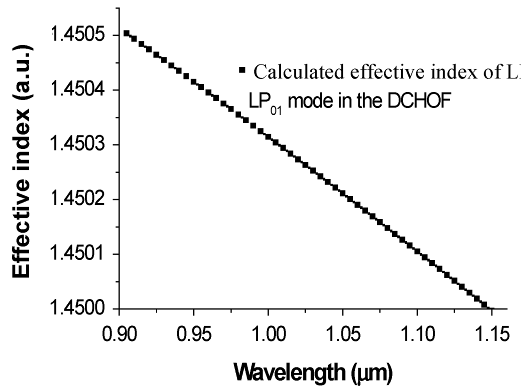

(a)

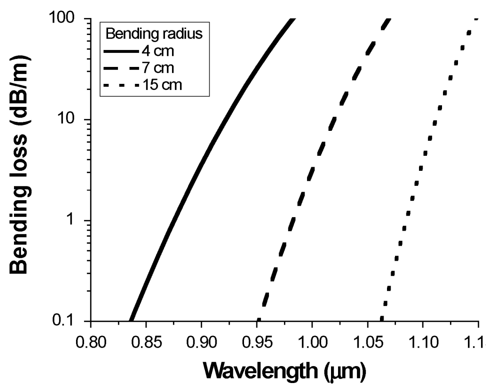

(b)

Fig. 5. (a) Calculated effective index of the fundamental LP_{01} mode versus wavelength for the DCHOF. (b) Bending loss versus wavelength at different bending radii of the DCHOF.

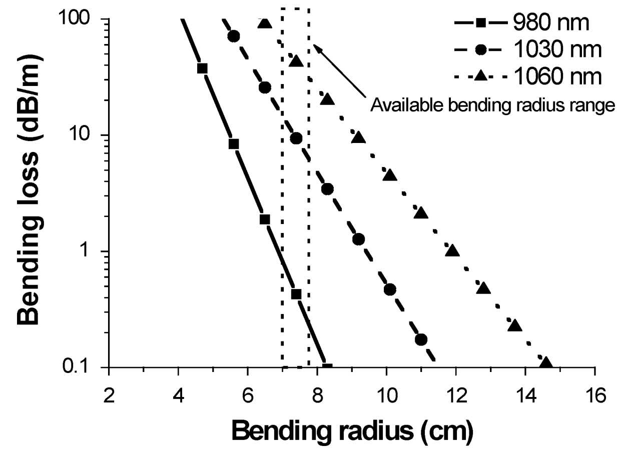

Fig. 6. Bending loss versus bending radius at three different wavelengths—980, 1030, and 1060 nm.

TABLE III
BENDING-LOSS VARIATION DEPENDING ON THE 2% TOLERANCE OF THE CORE THICKNESS

Core		Depressed clad		Hole radius (m)	Bending loss (dB/m) at 7cm bending radius		
Thickness (m)	NA	Thickness (m)	NA		980 nm	1030 nm	1060 nm
5.7 + 0.114	0.073	11.4	0.080	5	0.14	3.19	14.80
5.7					0.82	14.70	59.10
5.7 – 0.114					2.33	33.74	117.23

spectral filtering. Fig. 5(a) presents the effective index as a function of wavelength showing that the DCHOF has a theoretical fundamental mode cutoff at ~1150 nm. This behavior is important, as rapid change of the effective index with wavelength is needed to get spectrally sharp bending loss characteristics. Fig. 5(b) shows the calculated bending losses in the DCHOF at different bending radii. Experimentally, fibers are bent to a radius that provides the best output characteristics (typically the highest 980-nm output power). It suggests that ~7 cm is an appropriate bending radius that can induce a sufficient loss at 1030 nm.

We also calculated the bending loss as a function of the bending radius at three different wavelengths, 980 nm, 1030 nm, and 1060 nm, as shown in Fig. 6. The dotted rectangle indicates suitable bending radii for which over 10 dB/m of bending loss at both 1030 and 1060 nm can be induced, while the bending loss at 980 nm is small. Still the level of 980-nm loss is such that it will degrade the laser performance in fibers long enough (say, 6 m) to absorb the pump power. A spectrally sharper bending loss is desirable.

We must also consider tolerances in the fiber parameters. We have found that the fundamental mode cutoff is highly sensitive to the core thickness, more so than in a conventional fiber where the cutoff is proportional to the thickness. A change in cutoff may cause a significant variation in the bending loss. To investigate this, we varied the core thickness of 5.7 μm by $\pm$2%, and calculated the bending loss at a bending radius of 7 cm. Table III lists the results. A 2% variation causes a relatively big change in the bending loss at 980 nm, 1030 nm, and 1060 nm. However, it is possible to compensate variations in the core thickness and other core parameters by changing the bending radius. Then, the sharpness of the filter remains almost unaffected by a small change in core thickness.

IV. EXPERIMENTS AND RESULTS

We fabricated an Yb-doped DCHOF preform using the modified chemical vapor deposition (MCVD) and solution doping technique [11]. At the final collapsing stage, a hole of 0.5-mm diameter was left in the preform, which was then milled to a "double D" shape to improve the pump absorption by breaking the circular symmetry [12]. The preform was then drawn to a fiber with 120-μm inner-cladding diameter and coated with a low-index polymer outer cladding, which provided a nominal inner-cladding NA of 0.48. To reiterate, the Yb concentration was ~1500 ppm by weight. The drawn fiber has a central air hole diameter of 10 μm with a ring shaped Yb-doped aluminosilicate core and a depressed inner-cladding section of thicknesses 5.7 and 11 μm, respectively. The core and the depressed cladding index differences were 0.0016 ($NA_{co} = 0.073$) and -0.002 ($NA_{dip} = 0.080$) respectively, both with respect to

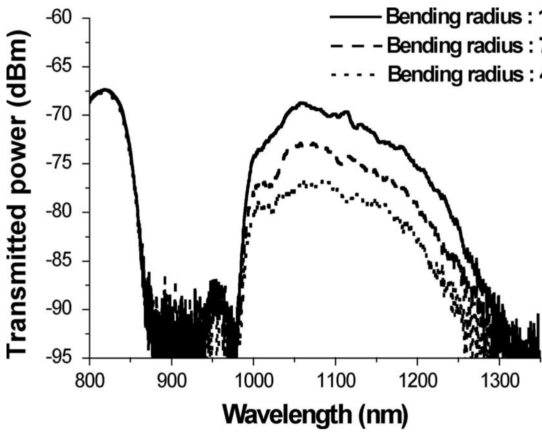

Fig. 7. Transmitted spectra of the fabricated Yb:Al-doped DCHOF at different bending radii measured with a spectrally flat white light source.

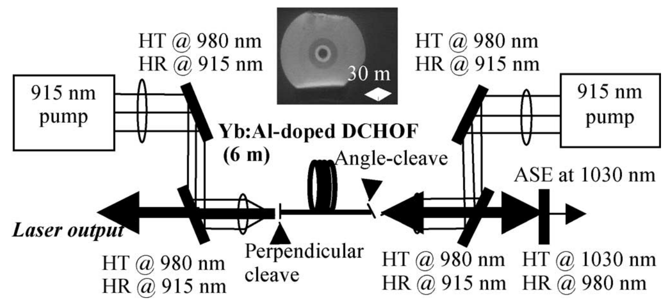

Fig. 8. Configuration of 980-nm Yb:Al-doped DCHOF laser. HT: high transmission; HR: high reflectivity; ASE: amplified stimulated emission.

the silica inner cladding. The low-power pump absorption was 1.3 dB/m.

The LP_{01} mode cutoff behavior of the fabricated DCHOF was verified by measuring the transmission spectrum with a spectrally flat white light source. For this measurement, both ends of the DCHOF were collapsed, and then spliced to single mode fiber (SMF) in order to remove the cladding modes guided in the inner cladding. Fig. 7 shows the transmission spectra of a 50-cm-long Yb-doped DCHOF for bend radii of 15, 7, and 4 cm. Based on the calculated results, it can be assumed that the bending loss can be so low as to be ignored at the bending radius of 15 cm for wavelengths shorter than 1030 nm.

The performance depends strongly on the loss at 980 nm. Unfortunately, the Yb absorption prevents us from measuring the bending loss around 980 nm. However, if we compare the experimental bending loss to the theoretical one of Fig. 5(b), the experimental filter characteristics are less sharp. Since bending loss depends strongly on fiber parameters, the difference is not surprising but the less sharp characteristics are a concern nonetheless. Differences might be due to discrepancies in the core refractive index profile and mode coupling. Furthermore, in a double clad fiber, the light remains guided by the inner cladding even beyond the (effective) fundamental mode cutoff wavelength and can be captured back by the core. In particular, any backcaptured light would influence the result more at small bend radii with theoretically very high bending loss and it would reduce the sharpness of the filter. However, with non-double-clad fibers also, we generally find that the experimental bending loss spectrum is less sharp than the theoretical one.

We can use the measured and calculated bending losses with 7-cm bending radius at 1030 nm to more reliably estimate the actual bending loss at 980 nm than the theoretical calculations of Figs. 5 and 6. A value of 0.82 dB/m is thus, predicted that is high enough to significantly degrade the efficiency. We conclude that it is not clear if the measured filter characteristics are sufficiently sharp for efficient high-power 980-nm operation. Rather, this has to be determined by laser experiments. The bending of the fiber should then be adjusted during laser operation to obtain the best combination of loss at 980 nm and 1030 nm.

We assessed laser performance at 980 nm in a conventional laser configuration, shown in Fig. 8 together with an end facet image of the fabricated DCHOF. A 6-m-long fiber was pumped by two multimode laser diode sources of relatively low brightness, with 200-μm 0.2-NA fiber pigtails. Up to a total pump power of 19 W was launched into the YDF through both of its ends via a combination of lenses and dichroic mirrors (DMs). A laser cavity was formed between a perpendicularly cleaved fiber end facet (4% Fresnel reflection) at the out-coupling end of the fiber and an external lens-coupled DM, which is highly reflective (HR) at 980 nm and highly transmissive (HT) at 1030 nm, at the other end of the fiber. The bending radius of the DCHOF was varied between 7 and 4 cm in order to find the maximum output power at 980 nm. We fixed the bending radius at 6 cm, which yielded the maximum output power at 980 nm. The single-pass pump absorption was 8 dB. It is calculated using the measured data of the input and output pump power in a single pass of pump light through the fiber.

The 980-nm laser characteristics are shown in Fig. 9. The maximum output power was 3.1 W with 34% slope efficiency (η) and 9.2-W threshold power, both with respect to the launched pump power. The relatively low slope efficiency can perhaps be explained by an undesirably high bending loss at 980 nm. Quenching is another possibility. Although the Yb concentration is relatively low, the YDFL operating at 980 nm is very sensitive to Yb quenching [7]. The slope efficiency will be discussed later in detail. On the other hand, the measured threshold is in good agreement with the theoretical value. Nevertheless, it is still quite high, which further degrades the overall efficiency.

At this stage the output was ring-shaped. We then collapsed the out-coupling end of the fiber and measured the beam quality. The power penalty from collapsing the fiber was less than 5%. An M^2 value of 1.09 was obtained, implying that the output beam was single-moded and nearly diffraction limited. Compared to our earlier results using a JAC fiber structure [6], this fiber has a larger inner-cladding area. Although the large inner-cladding results in a much higher 980-nm laser threshold, it does allow for pumping with standard pig-tailed multimode single-emitter laser diodes of relatively low brightness. Higher power pump sources of higher brightness, including commercially available pig-tailed diode bars and multiemitter sources as well as single or even multiemitter sources combined in commercially available tapered fiber bundles, should allow our fiber to be power-scaled well beyond the 10-W level.

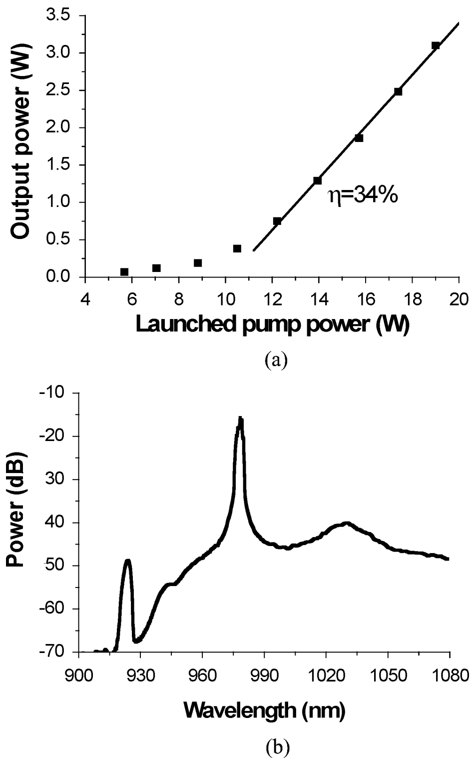

Fig. 9. Characteristics of 980-nm DCHOF laser. (a) Output power versus launched pump power. (b) Optical output spectrum (resolution 1 nm).

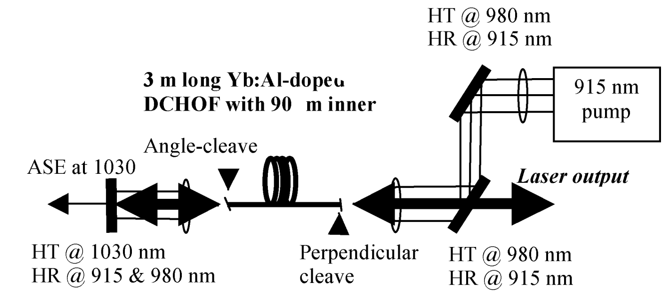

Fig. 10. Configuration of 980-nm laser based on Yb:Al-doped DCHOF with 90-μm inner-cladding diameter. HT: high transmission; HR: high reflectivity; ASE: amplified stimulated emission.

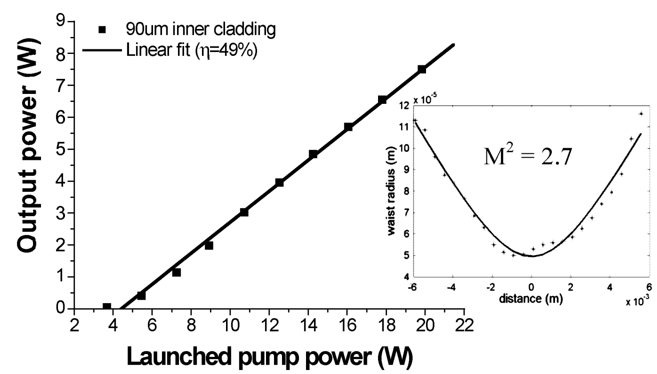

Fig. 11. Laser output characteristics of 980-nm YDFL based on 90-μm-thick Yb:Al-doped DCHOF. Inset: beam quality measurement data (M^2 value).

In order to increase the 980-nm output power, we investigated the use of a smaller inner-cladding fiber. This reduces the laser threshold, and allows us to use a shorter fiber that is less sensitive to the loss at 980 nm. The remainder of the preform used for the previous 120-μm diameter fiber was etched in a bath of Hydrofluoric acid to reduce the outer diameter only. The preform was then milled to a double D-shape and drawn to a 90-μm-diameter fiber to match the core parameters of the 120-μm-diameter fiber, but with an inner-cladding area that is $\sim$44% smaller. Fig. 10 shows the laser configuration used for the 90-μm fiber. The increased cladding-to-core area ratio led to an increased pump absorption. The fiber was, therefore, shortened to 3 m. It was pumped from one end using a 915-nm multimode diode, which delivers a maximum power of 32 W from a 100-μm 0.4-NA fiber. The maximum launched pump power was 19 W. As before, a laser cavity was formed between a perpendicularly cleaved end facet (4% Fresnel reflection) of the fiber and a 980-nm-HR 1030-nm-HT DM. This also reflects back the residual pump into the fiber, so that the pump was double-passed through the fiber. The fiber was coiled to an optimum radius of 6 cm, which again resulted in the highest output power. The maximum 980-nm power obtained was 7.5 W with 49% slope efficiency with respect to launched pump power (Fig. 11), i.e., higher than in the larger (120 μm) inner-cladding fiber. Furthermore, the threshold reduced to 4.2 W of launched pump power, i.e., 54% lower than the value for the thicker fiber. The beam quality was measured after collapsing the pump launch end of the fiber, and an M^2 of 2.7 was obtained. Compared to the 120-μm diameter fiber result, the beam quality was degraded in this case, even though the core size and NA in both fibers were the same.

We next discuss the reasons for these differences in output power and beam quality between the 90- and 120-μm-diameter fibers. The degraded beam quality can either be a result of lasing on cladding-modes or of a leakage of 980-nm laser radiation propagating in the core into the inner cladding. Such leakage can result from bending, since with a double-clad fiber, light lost from the core through bending would actually remain guided by the inner cladding. Even though the core parameters are similar for the 90- and 120-μm-diameter fibers, the increased microbending of a thinner fiber could lead to such differences in the bending losses of the core-mode between the two fibers. In order to further investigate the reasons for the degraded beam quality, we performed additional laser experiments with the 90-μm-diameter fiber, and used a pinhole to separate the light guided in the core and in the inner cladding. In this case, the laser cavity was formed between a perpendicularly cleaved end facet of the DCHOF fiber and a bulk grating with 60% first-order diffraction efficiency in a Littrow configuration. Both fiber ends were collapsed. Here, the residual pump was not relaunched back into the fiber. The fiber length used was 1.5 m. As long as the fiber is the same, we expect a similar behavior of the beam quality for the different laser configurations we used, despite the differences between the configurations. The output powers were measured before and after the pinhole. The results are shown in Fig. 12. The maximum output power was 3.2 W before the pinhole, with a slope efficiency η of 49% with respect

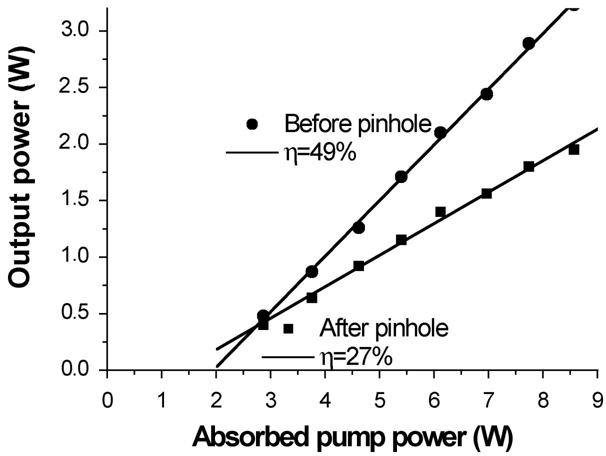

Fig. 12. Output power characteristics of a 980-nm Yb-doped DCHOF laser (90-μm diameter) before pinhole and after pinhole.

to the absorbed pump power. The beam propagation parameter M^2 was 2.7. After the pinhole, the maximum power obtained was 1.95 W with $\eta \sim 27\%$ and M^2 value of 1.28. Significantly, at low powers, there is no difference in output power between the two cases, which shows that the laser is (nearly) diffraction-limited. We conclude that bend-induced light leakage from the core into the cladding alone does not explain the degradation in beam quality, since this would be a largely power-independent process. Rather, there must be direct amplification of light propagating in cladding-modes, as a result of high gain in areas of the core that are not saturated by the lasing core-mode under high-power pumping. Some of the cladding-modes must have a significant overlap with such high-gain regions. The power transfer that results from the amplification (i.e., the stimulated emission), can either be in the form of cladding-mode lasing, or through amplification of light that has leaked out from the lasing core-mode. Since we have significant feedback at 980 nm, the gain required for cladding-mode lasing is expected to be lower than that required to amplify light leaked from the core mode to high power. This would indicate that cladding-mode lasing is the cause of the degraded beam quality. However, if the leakage from the core mode is sufficiently high into high-gain cladding-modes, this need not be the case. Further experiments, e.g., with mode-selective feedback, would be needed to clarify this. In any case, the significantly lower confinement of the cladding-modes would explain why the cladding-modes of the 120-μm-diameter fiber are not significantly excited. We note also, that the lack of excited cladding-modes in the 120-μm fiber implies that the leakage of light from the core to the cladding at 980 nm is small. Thus, the bending-loss for the core-mode at 980 nm must be relatively small.

We next consider the relatively low slope efficiency we obtain, and the higher efficiency of the 90-μm fiber. There are few possible explanations to this. As bending only couples light from the core to the inner cladding, bending-loss cannot explain the low efficiency. Furthermore, if bending-loss was anyway a significant loss mechanism, it would have to lead to large amounts of light emitted from the sides of the fiber, since the light is not detected at the ends of the fiber. This was not observed. Another possibility would be that pump power absorbed in regions of the core where the modal field of the core mode is weak cannot be transferred efficiently to the 980-nm laser field. However the low saturation intensity of Yb at 980 nm rules out this explanation, as in [7]. (Note that by contrast, it is still possible for the gain to reach high values in such regions.) The most likely explanation seems to be quenching of Yb-ions, which can severely impact the efficiency of cladding-pumped 980-nm YDFLs [7], [13].

The efficiency of the core-mode lasing of the 90-μm fiber (27% in Fig. 12) is similar to that obtained with the 120-μm mode fiber, emitting only from the core-mode (34% in Fig. 9). Note that while the 34% refers to launched power, the pump absorption is $\sim$90%; so the value for the efficiency with respect to the absorbed power is similar, or approximately 37%. The lower efficiency of the core-mode of the 90-μm fiber may be due to pump power transfer to competing cladding modes, when they start to lase. If so, this indicates that a fraction (37%–27%)/37% = 27% of the absorbed pump power is used for stimulated emission of the cladding-modes rather than the core-modes. From Fig. 11, a slope efficiency for cladding-modes of 22% with respect to all of the absorbed pump power can be inferred. This would correspond to a slope efficiency of 22%/27% = 81%, with respect to the 27% of the pump power that is available for cladding-pump lasing. Although this is only a rough estimate, a much higher slope efficiency for cladding-mode lasing is in agreement with the quenching hypothesis, as cladding-modes with a small overlap with the Yb-doped core would be less impacted by Yb-quenching than the core-mode is [7]. Further characterization, e.g., of unsaturable absorption [13], would be needed to firmly establish the impact of quenching in our fiber.

V. Conclusion

We have demonstrated an Yb:Al-doped silica DCHOF with nonzero fundamental mode cutoff for high-power cladding-pumped 980-nm laser operation. Such fibers act as short-pass filters that allow longer wavelengths to be suppressed. We have analyzed the requirements of a cladding-pumped 980-nm fiber laser, in particular, the need to suppress competing emission at 1030 nm and longer wavelengths, and the ability of DCHOFs of different designs to satisfy these requirements. We find that even though the 980-nm emission in the Yb-system is quite close to the competing emission, which normally dominates in a cladding-pumped fiber, it is still possible to design the DCHOF to efficiently suppress the competing emission. Experimentally, we obtained 3.1 W of output power in a nearly diffraction limited beam (M^2 value of 1.09) in a fiber with a 120-μm inner-cladding diameter, a laser threshold of 9.2 W, and a slope efficiency of 34%. The large inner cladding facilitates pumping with conventional commercially available pump diodes, but it also leads to a high threshold. The output power was increased to 7.5 W when the inner-cladding diameter was reduced to 90 μm while keeping the core parameters constant, as a result of a lower threshold as well as a higher slope efficiency. However, at the same time, the beam quality degraded to an M^2 value of 2.7. We attribute this to cladding-mode lasing in the thinner fiber with its larger overlap between cladding-modes and the core. In an improved fiber design, cladding-modes can be suppressed by a 980-nm absorber in the cladding. The relatively low slope efficiency is attributed to quenching, which can be avoided with improved fabrication [7].

A cladding-diameter of 90–100 μm is still compatible with standard low-cost diode sources. Thus, our result suggests that the DCHOF approach can be used for low-cost single-mode 980-nm laser sources with a few watts of output power pumped by single-emitter multimode diodes with $\sim$10 W of output power. It would also allow for scaling of the power to above 10 W with commercially available multidiode and multiemitter diode sources including diode bars.

REFERENCES

[1] L. A. Zenteno, J. D. Minelly, A. Liu *et al.*, "1 W single-transverse-mode Yb-doped double-clad fibre laser at 978 nm," *Electron. Lett.*, vol. 37, pp. 819–820, 2001.

[2] L. B. Fu, R. Selvas, M. Ibsen *et al.*, "Fiber-DFB laser array pumped with a single 1 W CW Yb-fiber laser," *IEEE Photon. Technol. Lett.*, vol. 15, no. 5, pp. 655–657, May 2003.

[3] V. Prosentsov, E. Sherman, A. Patlakh, Y. Ariel, and D. Eger, "Efficient Yb-doped air-clad fiber laser operating at 980 nm and its frequency doubling," *Proc. SPIE*, vol. 4974, pp. 193–201, 2003.

[4] D. B. S. Soh, C. Codemard, S. Wang *et al.*, "A 980 nm Yb-doped fiber MOPA source and its frequency doubling," *IEEE Photon. Technol. Lett.*, vol. 16, no. 4, pp. 1032–1034, Apr. 2004.

[5] A. Bouchier, G. Lucas-Leclin, and P. Georges, "Single-mode Yb-doped fiber laser at 980 nm for efficient frequency-doubling," in *Proc. Conf. Lasers Electro-Opt. Eur.*, Munich, Germany, Jun. 12–17, 2005, pp. 1195–1197.

[6] K. H. Ylä-Jarkko R. Selvas, D. B. S. Soh *et al.*, "A 3.5 W 977 nm cladding-pumped. jacketed-air clad ytterbium-doped fiber laser," in *Advanced Solid State Photon. 2003*, J. J. Zayhowski, Ed. Washington, DC: Optical Society of America, 2003, pp. 103–107.

[7] J. Nilsson, J. D. Minelly, R. Paschotta, D. C. Hanna, and A. C. Tropper, "Ring-doped cladding-pumped single-mode three-level fiber laser," *Opt. Lett.*, vol. 23, pp. 355–357, 1998.

[8] J. Kim, P. Dupriez, D. B. S. Soh, J. Nilsson, and J. K. Sahu, "Nd:Al-doped depressed clad hollow fiber laser at 930 nm," presented at the Adv. Solid State Photon. 2005 Tech. Dig. CD-ROM. Washington, DC, 5, Optical Society of America, Paper MC5.

[9] J. Kim, P. Dupriez, D. B. S. Soh, J. Nilsson, and J. K. Sahu, "Core area scaling of Nd:Al-doped silica depressed clad hollow optical fiber and Q-switched laser operation at 0.9 mm," *Opt. Lett.*, vol. 31, pp. 2833–2835, 2006.

[10] J. I. Sakai and T. Kimura, "Bending loss of propagation modes in arbitrary-index profile optical fibers," *Appl. Opt.*, vol. 17, pp. 1499–1506, 1978.

[11] J. E. Townsend, S. B. Poole, and D. N. Payne, "Solution doping technique for fabrication of rare-earth doped optical fibers," *Elec. Lett.*, vol. 23, pp. 329–331, 1987.

[12] D. Kouznetsov, J. V. Moloney, and E. M. Wright, "Efficiency of pump absorption in double-clad fiber amplifiers II: Broken circular symmetry," *J. Opt. Soc. Am. B*, vol. 19, pp. 1259–1263, 2002.

[13] R. Paschotta, J. Nilsson, P. R. Barber, J. E. Caplen, A. C. Tropper, and D. C. Hanna, "Lifetime quenching in Yb doped fibers," *Opt. Commun.*, vol. 136, pp. 375–378, 1997.

[14] R. Selvas, J. K. Sahu, and J. Nilsson, "Q-switched 980 nm Yb-doped fiber laser," presented at the Conf. Lasers Electro-Opt., Tech. Dig. Washington, DC: Optical Society of America, 2002, pp. 565–566.

J. Kim received the B.Sc. and M.Sc. degrees in inorganic material engineering from Hanyang University, Seoul, Korea, in 1999 and 2001, respectively.

In 2001, he joined the Fiber Optic and Telecommunication Research Center, LG Cable, Korea, as a Research Engineer. Currently, he is working toward the Ph.D. degree from the Optoelectronics Research Centre, University of Southampton, Southampton, U.K. His current research interests include the design and fabrication of rare-earth-doped fibers using MCVD tents.

Daniel B. S. Soh received the B.Sc. and M.Sc. degrees in electrical engineering from Seoul National University, Seoul, Korea, and the Ph.D. degree from the University of Southampton, Southampton, U.K., in 1997, 1999, and 2005, respectively.

In 2006, he was a Postdoctoral Research Fellow at the University of California, Berkeley, CA, for one year. Then, he joined Calmar Optcom Inc., Sunnyvale, CA, in 2006. Currently, he is an R&D Manager with the Optoelectronics Research Centre, University of Southampton. His current research interests include femtosecond lasers, high-power fiber lasers and amplifiers, and theory of nonlinear fiber optics. He is the author of more than 40 technical papers and is a holder of several patents.

Johan Nilsson received the Ph.D. degree in engineering science from the Royal Institute of Technology, Stockholm, Sweden, in 1994.

He is a Professor at the Optoelectronics Research Centre (ORC), University of Southampton, Southampton, U.K., since 1998. He is a Consultant to SPI Lasers. He is also the Vice Chair of the laser science and engineering group of the Optical Society of America's (OSA's) Science and Engineering Council. His current research interests include device, system, fabrication, and material aspects of high-power fiber sources and erbium-doped fiber amplifiers, as well as their applications. He has published over 200 scientific papers, including many invited and postdeadline papers at leading international conference proceedings.

Dr. Nilsson is a member of OSA. He serves on the technical program committees of the Optical Fiber Communication Conference, the Fiber Laser Systems Technology and Applications Conference at Photonics West, and the Frontier in Optics Conference.

David J. Richardson was born in Southampton, U.K., in 1964. He received the B.Sc. and Ph.D. degrees in fundamental physics from Sussex University, Sussex, U.K., in 1985 and 1989, respectively.

In 1989, he joined the Optoelectronics Research Centre, University of Southampton, Southampton, U.K., as a Research Fellow where he is currently a Deputy Director, responsible for its Optical Fiber Devices and Systems Division. His current research interests include holey fibers, high-power fiber lasers, short pulse generation, nonlinear optics and high-capacity optical communications systems. He is the author of more than 500 journals and conference proceeding papers. He is the holder of over 20 patents. He is the cofounder of Southampton Photonics Incorporated.

Jayanta K. Sahu received the Ph.D. degree in physics from the India Institute of Technology (IIT), Kharagpur, India, in 1997.

In 1992, he became a Research Scientist at IIT, Kharagpur. In May 2000, he joined the silica fiber fabrication group at the Optoelectronics Research Centre (ORC), University of Southampton, Southampton, U.K., where he is currently a Principal Research Fellow. In 2005, he received a UKRC Robert's (Academic) Fellowship. His current research interests include optical materials, development of novel silica-based fiber structures using MCVD, and cladding-pumped rare-earth-doped fiber lasers and amplifiers. He has published over 150 papers in scientific journals and conference proceedings.